Physical constraints on thermoregulation and flight drive morphological evolution in bats

Juan G. Rubalcaba[a,b,1] (ID), Sidney F. Gouveia[c] (ID), Fabricio Villalobos[d] (ID), Ariovaldo P. Cruz-Neto[e], Mario G. Castro[b], Talita F. Amado[b] (ID), Pablo A. Martinez[f], Carlos A. Navas[g] (ID), Ricardo Dobrovolski[h], José Alexandre Felizola Diniz-Filho[i], and Miguel Á. Olalla-Tárraga[b] (ID)

Body size and shape fundamentally determine organismal energy requirements by modulating heat and mass exchange with the environment and the costs of locomotion, thermoregulation, and maintenance. Ecologists have long used the physical linkage between morphology and energy balance to explain why the body size and shape of many organisms vary across climatic gradients, e.g., why larger endotherms are more common in colder regions. However, few modeling exercises have aimed at investigating this link from first principles. Body size evolution in bats contrasts with the patterns observed in other endotherms, probably because physical constraints on flight limit morphological adaptations. Here, we develop a biophysical model based on heat transfer and aerodynamic principles to investigate energy constraints on morphological evolution in bats. Our biophysical model predicts that the energy costs of thermoregulation and flight, respectively, impose upper and lower limits on the relationship of wing surface area to body mass (S-MR), giving rise to an optimal S-MR at which both energy costs are minimized. A comparative analysis of 278 species of bats supports the model's prediction that S-MR evolves toward an optimal shape and that the strength of selection is higher among species experiencing greater energy demands for thermoregulation in cold climates. Our study suggests that energy costs modulate the mode of morphological evolution in bats—hence shedding light on a long-standing debate over bats' conformity to ecogeographical patterns observed in other mammals—and offers a procedure for investigating complex macroecological patterns from first principles.

biophysical model | thermoregulation | Chiroptera | bat | Bergmann's rule

Body size and shape determine how organisms exchange heat and mass with their environment, defining their metabolic requirements and costs of locomotion (1–4). To gain insight into the drivers of body size evolution and its patterns of variation across spatial and environmental gradients, we need a thorough understanding of the mechanisms driving these patterns. The mechanisms linking body size and energy balances are grounded on the physics of heat and mass transfer, biomechanics, and physiology (5). Therefore, physical processes governing these energy exchanges may be critical to understanding how animal morphology evolves and responds to environmental changes (6–9).

The idea that physical mechanisms linking body size and energy balance scale up into ecogeographical patterns dates back to the 19th century when Carl Bergmann postulated that larger endotherms would be more common in colder regions, whereas smaller endotherms would predominate in warmer environments (10). The original explanation for this so-called Bergmann's rule is that increasing body size decreases the surface area-to-volume ratio and thus reduces heat dissipation rates and costs of thermoregulation (11, 12). When this notion is applied to body appendages such as legs, wings, or tails, endotherms living in colder regions are expected to evolve shorter limbs, reducing their surface-to-volume ratio—a prediction known as Allen's rule (13). Observed patterns of body and limb size variation across latitudinal or environmental temperature gradients support Bergmann's and Allen's rules in birds and mammals worldwide (11, 12, 14). However, the generality of these rules remains under debate. For instance, controversy exists on whether these ecogeographical rules should be interpreted either as intra- or interspecific patterns (15, 16) and on whether heat conservation is the most relevant mechanism underpinning variations in body size and shape (12, 17–19). Thus, the validity of Bergmann's and Allen's rules has been questioned for some taxa such as bats (20–24), for which morphological evolution is thought to be primarily driven by selective forces acting to maximize flight performance rather than heat conservation (25, 26).

Among mammals, bats are subject to unique selective pressures on body size and shape (25–27). Contrary to nonvolant mammals, the highly vascularized, naked wing membranes of bats increase their surface-to-mass ratio and the rate of heat dissipation

Significance

Energetic constraints of flight and thermoregulation have long been thought to explain why most bat species are small and live predominantly in warm latitudes. We use physical models to investigate how body size, wing shape, and climate modulate these energetic constraints. Our model predicts that thermoregulatory and flight costs, respectively, impose upper and lower bounds on the wing surface-to-mass ratio, giving rise to an optimum shape, and that variations around this optimum are more constrained in cold regions. A comparative analysis across bat species supports the model's predictions, suggesting that body shape evolves toward an optimum with stronger selective pressures in cold regions. The model and data together suggest that thermoregulatory and locomotory constraints modulate the evolution of bats' morphology.

during flight (28–31). Furthermore, the amount of energy required to power flight is much higher than that required for terrestrial locomotion, imposing constraints on both body size and shape (27, 32, 33). Compared with birds, bats exhibit morphological and metabolic constraints inherent to their mammalian structure, such as a less efficient ventilatory system, lower flight muscle mass, and naked wings that further constrain energy utilization and morphology (34). The combined influence of thermoregulatory and locomotory constraints on bats' morphology can determine how body size evolves, particularly in response to environmental factors such as temperature. A better understanding of the ecological and evolutionary processes shaping bats' morphology requires knowledge of the mechanisms linking body size, heat balance, and locomotion. So far, the combined costs of thermoregulation and locomotion and their effects on morphological evolution remain largely unexplored.

Here, we investigate how body size and shape determine the energy costs of thermoregulation and flight in bats combining principles of thermodynamics and aerodynamics. We built upon biophysical models of nonvolant mammals (35, 36) to incorporate the impact of heat dissipation through the wings and the energy costs of flight on the overall energy balance (37–40). We used a heat transfer model to calculate how body size and wing surface area affect the rate of heat exchange with the environment and thereby the amount of energy required to maintain high and stable body temperature (Fig. 1). The model combines resistances to heat dissipation exerted by body tissues, the insulating layer of fur, convective, and radiative heat exchange (36), as well as heat dissipation through the wing surface (*Methods*). Using an aerodynamic model, we also calculated how body mass and wing surface area influence the amount of energy required to oppose weight and drag forces at flight and the heat generated as a by-product of flapping (38–40). We used these estimations to predict how energy costs of thermoregulation and flight change in response to variations in the relationship of wing surface to body mass. Then, we investigated whether changes in wing surface-to-mass ratio in response to temperature can minimize these costs—thus testing the validity of Bergmann's and Allen's rules in bats. Using morphological data of 278 species of bats, we tested models' predictions on how wing surface area-to-mass ratio varies with the environmental temperature.

Results and Discussion

Energy Constraints on Body and Wing Size. As the wing surface area increases for a given body mass, the higher wing surface-to-body mass ratio (S-MR) accelerates heat dissipation rates, thereby increasing the amount of energy required for thermoregulation (Fig. 2*A*). Conversely, a larger wing surface area reduces the mechanical power required for flapping, thus reducing energy requirements for flight. A similar pattern occurs when varying body mass while leaving wing surface area constant (Fig. 2*B*). In that case, the costs of thermoregulation increase with decreasing body mass, whereas the costs of flight increase toward larger masses. When the energy requirements for thermoregulation and flight are modeled across different combinations of body masses and wing surface areas, the resulting coordinate plane shows that both energy costs vary primarily in relation to the S-MR (Fig. 2*C*). The S-MR is proportional to the ratio of heat dissipation to heat production and both Bergmann's and Allen's rules are defined in terms of this ratio, i.e., endothermic animals living in colder environments are expected to evolutionarily reduce the ratio of heat dissipation to production either via increasing body size (Bergmann's rule) or via reducing appendage size (Allen's rule). Because we are interested in the relationship between energy requirements and S-MR, we reduced the dimension of the plane in Fig. 2*C* by computing the energy costs across the line with slope −1 passing through the modal wing surface area and the modal body mass of bat species, which represents the variation in energy costs in relation to S-MR for the typical bat morphology. This dimensional reduction shows that the total energy requirements (the sum of the energy costs of thermoregulation and flight) display a U-shaped curve in relation to the S-MR, with a minimum at approximately −7.27 (i.e., 6.96 cm$^2 \cdot$g^{-1}; Fig. 2*D*; see also *SI Appendix,* section 3). Thus,
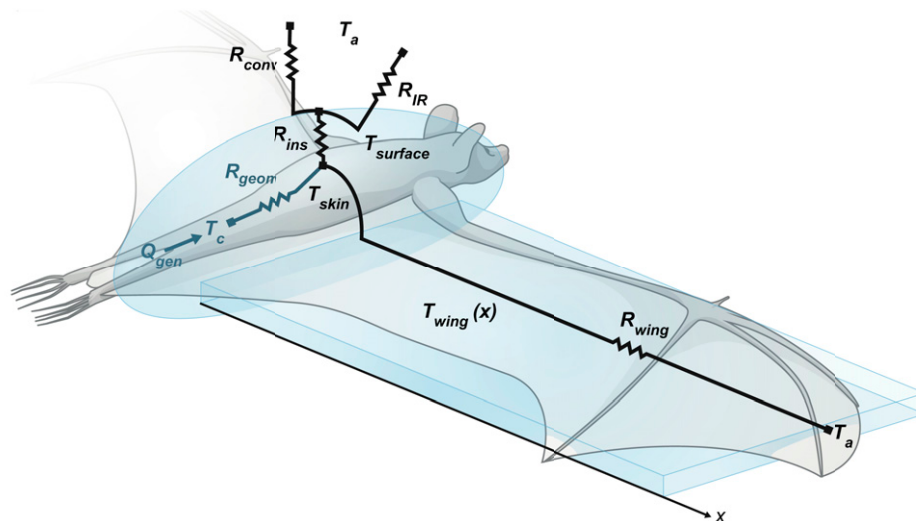

Fig. 1. Diagram of the heat transfer model used to simulate the costs of thermoregulation, i.e., the amount of heat, Q_{gen}, required to maintain constant core body temperature, T_c, at a given ambient temperature, T_a. Heat dissipation is modeled using a network of resistors representing the body geometry, R_{geom}, insulating fur layer, R_{ins}, the boundary layer of air in direct contact with the body, R_{conv}, the balance of emitted and absorbed long-wave radiation, R_{IR}, and geometry of the wings, R_{wing}. This combination of resistors determines heat dissipation from the body core, as well as the skin, T_{skin}, and body surface temperatures, $T_{surface}$. Finally, wing temperature, $T_{wing}(x)$, declines from the base, where it matches T_{skin}, to the wing tip, determining the overall heat dissipation rate from the wing surface.
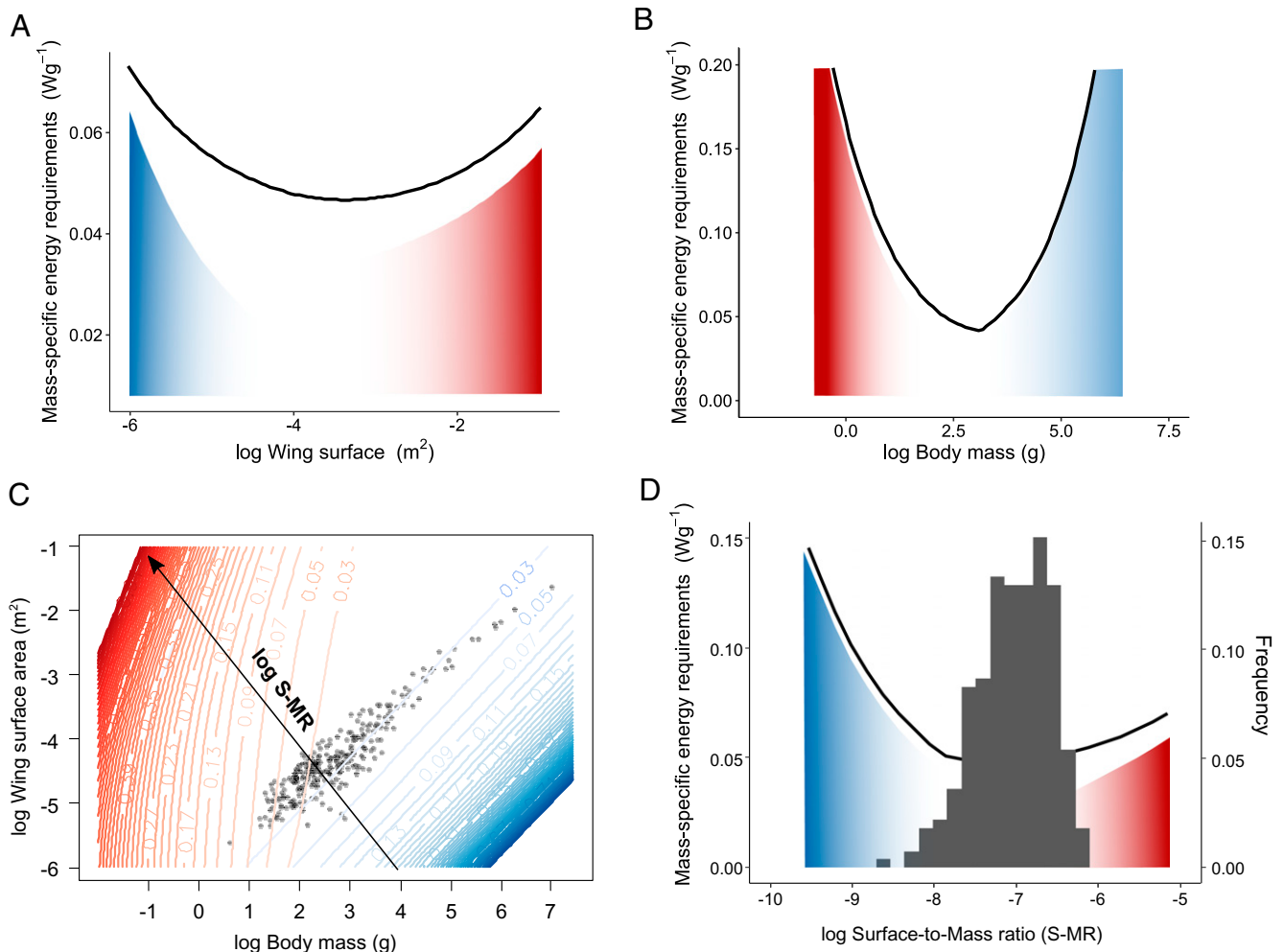
Fig. 2. Predicted energy requirements for flight (blue shading), thermoregulation (red shading), and total energy (black lines; flight + thermoregulation) in relation to wing surface area for a 10-g bat (*A*), and in relation to body mass, keeping wing surface area constant at 120 cm² (*B*). The coordinate plane (*C*) represents energy requirements across different combinations of wing surface area and body mass. The black arrow represents the change in S-MR across the modal wing surface area and body mass of bat species, which was used to represent the variation in energy requirements as a function of S-MR (ordinate axis in *D*). The energy costs of thermoregulation are predicted to be higher among species with high S-MR, while the costs of flight increase with decreasing S-MR (*D*). These analyses use a constant environmental temperature of 25 °C.

our model suggests that the energy costs of thermoregulation and flight are similar in magnitude and may impose, respectively, upper and lower bounds on S-MR (Fig. 2*D*).

Based on the premise that evolution favors morphologies that minimize energy costs such as those of locomotion and thermoregulation (37, 41), we predict that the modal S-MR of bats should be close to the value at which mass-specific energy requirements are minimum. To test this prediction, we compared wing surface areas, body masses, and S-MR of 278 bat species with the predicted energy costs at 25 °C (i.e., the modal temperature across their geographical ranges; see *Data Collection and Analyses*). We found that most species occur in the region where energy requirements are predicted to be minimum (Fig. 2*C*), although the mass scaling of wing surface area does not seem to follow the diagonal at which total costs are minimized. This result suggests that the model captures the relationship between energy and S-MR for the most typical (modal) morphology of bats but not the actual mass scaling of wing surface area. When the energy costs are analyzed in relation to S-MR, the observed distribution of S-MR falls within the range where energy costs are minimum (Fig. 2*D*). Thus, the mean of the observed S-MR distribution is −6.95 (in natural log scale), ranging from −7.83 and −6.23 (5 to 95% quantiles), which is

close to the value at which energy costs of flight and thermoregulation are predicted to be minimized (−7.27; Fig. 3*A*). Therefore, the model describes how energy costs of thermoregulation and flight vary in relation to the S-MR and provides an estimation of the optimal S-MR that closely matches the average value observed in bats.

Energy Constraints and Temperature. To explore the influence of environmental temperature on the evolution of bat morphology, we computed the energy costs in relation to the S-MR across different environmental temperatures (Fig. 3*A*). As temperature decreases, the increased costs of thermoregulation could be compensated with a lower S-MR (e.g., increasing body mass while keeping wing surface constant), as predicted by Bergmann's rule. However, the costs of flight remain relatively invariant in relation to temperature and impose a lower limit on S-MR across the temperature gradient (Fig. 3*A*). Note that although a higher air temperature is also associated with a lower air density, which increases flight costs, the change in flight power with temperature is small when compared to the change in thermoregulatory requirements. This analysis suggests that S-MR is constrained across temperatures with lower and upper limits imposed, respectively, by the costs of flight
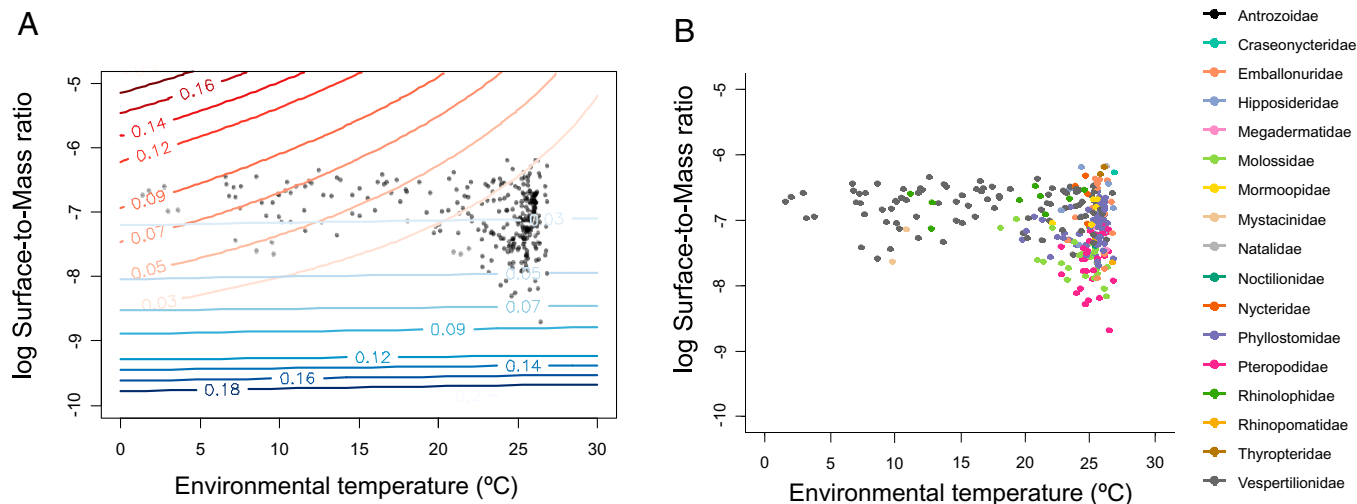
Fig. 3. Predicted requirements for thermoregulation (red shading) and flight (blue shading) relative to environmental temperature and for different wing surface-to-mass ratios (*A*). While a lower surface-to-body mass ratio allows reducing the costs of thermoregulation as temperature decreases, the costs of flight impose a lower limit. Thus, wing surface-to-mass ratios may be constrained across temperatures and display lower variability in cold regions. This relationship was compared with empirical data across 278 bat species (*B*).

and thermoregulation, and these constraints are stronger in cold (i.e., temperate) than in warm (i.e., tropical) environments (Fig. 3*A*). As temperature increases, the costs of thermoregulation become smaller, reducing physical constraints, and increasing the variance in SMR (Fig. 3*A*). Therefore, our model predicts that selective regimes on S-MR in bats change across temperatures, with stronger selection and lower variance in S-MR in cold than in warm environments (Fig. 3*A*).

To test the above predictions, we analyzed the mode of evolution of S-MR and how it varies among species living in warm and cold environments (see *Methods*). Specifically, we compared the likelihood that S-MR evolves either via Brownian motion (BM) or following an Ornstein–Uhlenbeck process (OU) with one or multiple selective regimes across temperatures (see *Methods*). Among all candidate evolutionary models, the OU model with multiple selective regimes was favored to explain the evolution of S-MR in bats (*SI Appendix*, Table S3). The best-fitting model showed that the strength of selection (parameter α of the OU model) is higher among species inhabiting cold environments, and the variance in S-MR, σ^2, is lower in colder than in warmer regions (Table 1). The observed optimal trait values, θ, are close to the optimum predicted by our biophysical model, although there is a tendency of θ to decrease toward warmer regions, contrary to the model's prediction (Table 1). Nonetheless, the linear relationship between S-MR and temperature (analyzed using phylogenetic generalized least squares) showed that this variation was not statistically significant ($\beta = 0.001$, $\lambda = 0.829$; $t = 0.37$, degrees of freedom = 276, $P = 0.708$; Fig. 3*B*), suggesting that the change in θ of the OU model was weak and potentially affected by the change in trait variance across temperatures. Altogether, these results

support the prediction of our biophysical model that selective regimes on S-MR vary across environmental temperatures, with stronger constraints (i.e., higher strength of selection) in colder than in warmer settings.

While most mammals experienced a burst of morphological variation early in their evolutionary history, followed by a slower change rate, bats' body mass was previously found to evolve toward an optimum value (26). Our model and empirical results suggest that the unique mode of evolution of bat morphology results from the combined costs on locomotion and thermoregulation. Thus, while the energy costs of thermoregulation may favor an adaptive reduction in S-MR in cold environments, e.g. via increasing body size or reducing wing surface area, the energy costs of flight may oppose to these reductions in S-MR and constrain its variation toward colder climates. Therefore, although the mechanisms driving Bergmann's and Allen's rules may also be present in bats, selective forces acting to reduce the cost of flight prevent bats from reducing their surface-to-volume ratio in cold environments. Hence, our model explains 1) why morphological evolution in bats follows an OU process, 2) why the selective pressure on S-MR is higher in cold than in warm environments, and 3) why S-MR does not vary significantly with temperature. These results shed light on a long-standing debate on the lack of conformity of bats to macroecological patterns in mammal body size (21–24).

Understanding how morphology and activity affect the thermoregulatory requirements of flying bats remains a challenge due to technical difficulties in assessing their body and wing temperature distributions and the heat exchange among different body structures during flight (42, 43). Our biophysical

Table 1. Results of the OU model for the evolution of wing S-MR in bats

Temperature range	Optimal S-MR value	Strength of selection	Evolutionary rate
Below 23 °C	$\theta_{cold} = -6.78$	$\alpha_{cold} = 0.057$	$\sigma^2_{cold} = 0.003$
23–25 °C	$\theta_{warm} = -7.01$	$\alpha_{warm} = 0.047$	$\sigma^2_{warm} = 0.010$
Above 25 °C	$\theta_{hot} = -7.12$	$\alpha_{hot} = 0.035$	$\sigma^2_{hot} = 0.035$

The model includes three attractors representing different selective regimes across environmental temperatures, each of which is characterized by an optimum surface-to-mass ratio (log scale), strength of selection. and evolutionary rate.

modeling approach provides a means to infer these energy requirements from morphological and environmental data. However, this approach has limitations because it focuses on a simplified geometry for the body and the wings and involves parameters that remain difficult to assess empirically such as the body and wings' thermal conductivity. Thus, the predicted relationships between energy demands and morphology and the predicted optimal wing surface-to-mass ratio are sensitive to variations in parameters related to heat conservation and heat conversion (*SI Appendix,* section 3). This dependence means that interspecific variation in functional traits involved in heat conservation may ultimately affect physical constraints on thermoregulatory demands. Using values for these parameters that are representative for bats (*SI Appendix,* Table S1), our approach captured general patterns such as the overall variation in the wing surface-to-mass ratio across bat species. However, a detailed version of the model, e.g. aimed at predicting thermal constraints for a particular species, should include more accurate descriptions of the body and wing geometry and specific measurements for the thermal conductivity and energy conversion coefficients. In addition, a more detailed version of the model should include a more accurate characterization of the thermal environment and information on environmental conditions such as humidity, which slightly influences air density and therefore the costs of flight.

Altogether, our model and results suggest that physical boundaries on thermoregulation and flight constrain the evolution of bat morphology, in which the wing surface-to-mass ratios undergo a strong selective constraint for minimizing both costs. Although morphological adaptations importantly determine both thermoregulation and flight costs, other traits can also evolve to reduce these costs. For instance, selective forces may act on the energy uptake and transport systems, increasing their capacity to meet the demands of flight muscles and thermogenic organs. A more effective energy uptake and transport systems may reduce the costs of thermoregulation and flight, relaxing the constraints on body size and shape. For example, birds have a more effective through-flow respiratory system, greater flight muscle mass than bats, and feathers that reduce heat dissipation through the wings. This specialization for flight reduces locomotion costs and permits birds to attain larger body sizes than bats (34). Behavioral and physiological strategies aimed at increasing energy uptake from food could also reduce the overall costs of thermoregulation and flight. For example, bats could feed on high-calorie diets to cope with higher energy demands and thus maintain small body sizes in cold environments. Alternatively, some bat species can reduce the costs of thermoregulation by voluntarily reducing body temperature to survive periods of food shortage and cold weather [i.e., torpor (44)]. Variations in food availability, e.g. pulses of insect availability in seasonal environments, can significantly influence energy supply and thus the relative importance of the predicted energy constraints. However, further empirical research is needed to understand the prevalence of these strategies and the proximate mechanisms linking, for example, diet type and thermogenic metabolism in bats (45, 46).

The evidence that the strength of selection on wing surface-to-mass ratio increases toward colder regions supports the idea that climatic conditions drive the overall patterns of morphological evolution in bats. Furthermore, this result suggests that strategies aimed at reducing physical constraints such as torpor may also incur costs or trade-offs, which ultimately limit the effectiveness of selection. Thus, the costs associated with these strategies, together with the constraints on morphological adaptations, suggest that bat species may be progressively more challenged in colder regions, which together with historical processes [e.g., phylogenetic conservatism of climatic niches (47, 48)] may explain why bat species richness strongly decays toward colder latitudes worldwide (49–51).

The role of climate on biogeographical and evolutionary patterns is primarily mediated by its effect on organismal physiology. Correlational approaches in macroecology and macroevolution have traditionally investigated the effect of climate by identifying the main climatic correlates of species' traits (e.g., body size and geographic ranges). Although such correlational procedures provide accurate statistical descriptions of ecogeographical patterns, they have limited capacity to infer their underpinning mechanisms because they mostly rely on information derived from the species' current geographic distributions (52). Emerging mechanistic models that predict physiological performance from environmental information do not rely on species' geographic ranges but rather simulate physiological performance in any possible location, based on first principles (e.g., refs. 36 and 52). Developing these models is challenging because they require information on complex, interacting physical and physiological mechanisms. Here we show that physical principles of heat transfer and aerodynamics can be combined to understand complex interactions between selective forces acting on locomotory and thermoregulatory performance in bats.

Methods

Modeling Bats' Energy Requirements. We modeled energy requirements for thermoregulation using a steady-state heat-exchange model. We used the electrical circuit analogy where the heat generated in the body for thermoregulation, Q_{gen} (watts) is transferred to the body surface powered by the gradient of temperature between the body core T_c (degrees Celsius) and the environment T_a (35, 36). This heat flow finds "resistance" due to the body geometry, R_{geom} (degrees Celsius per watt), and the insulating layer of fur, R_{ins}. At the body surface, resistance to heat dissipation occurs due to the convective, R_{conv}, and radiative, R_{IR}, heat exchange with the environment (*SI Appendix,* section 1 and refs. 28, 35, 36, and 53). In bats, heat transfer from the wing surface significantly influences the overall heat balance because wing membranes are highly vascularized, lack fur insulation, and experience high rates of forced convection at flight (28). Therefore, we included an additional resistance, R_{wings}, to describe how much heat is dissipated from the wings (*SI Appendix,* section 1). To characterize total thermal resistance, we considered that heat is dissipated in parallel (simultaneously) from the body, R_{body}, and from the wings, R_{wing}, and thus the expression for the total resistance is

$$R_{tot} = R_{geom} + \frac{R_{body}R_{wing}}{R_{body} + R_{wing}}$$
$$\text{with } R_{body} = R_{ins} + \frac{R_{conv}R_{IR}}{R_{conv} + R_{IR}}. \tag{1}$$

Applying the electrical circuit analogy, heat dissipation rate in endotherms is a function of the temperature gradient between the body core, T_c, and the environment, T_a, divided by the total resistance to heat transfer, R_{tot}. When modeling flying bats, we also need to consider that part of the heat generated as a by-product of flapping, Q_{flight}, increases body temperature, which may allow them to reduce heat production for thermoregulation, Q_{gen} (54). Thus, being α the proportion of by-product heat that can substitute for the heat required for thermoregulation, the thermogenic metabolic rate of a flying bat is

$$Q_{gen} = \frac{T_c - T_a}{R_{tot}} - \alpha Q_{flight}. \tag{2}$$

When the heat dissipation rate exceeds the basal metabolic rate (BMR), Q_{gen} rises above BMR to restore this heat and maintain body temperature constant. In contrast, Q_{gen} is equal to BMR when the heat dissipation rate is below BMR, which constitutes the lower bound of metabolism (36). From these considerations, heat dissipation results from both the body geometry [modeled as an

ellipsoid with an insulating layer of fur (36)] and wing geometry (modeled as rectangular extensions of the body). These simplifications are necessary to derive an analytical solution that relates heat dissipation with body size and shape. The geometry of the ellipsoidal body (semiaxis length, volume, and surface area) was calculated using allometric functions of body mass (*SI Appendix*, section 1). Therefore, when we compared model predictions with empirical data, we effectively assumed that body density does not change among species and wing weight is negligible (as empirical measurements of body mass in bats also include the wings). These simplifications allowed us to use body mass instead of volume as an indicator of body size, thus increasing the number of species for which empirical data were available.

To model mechanical power required for flapping and the by-product heat of muscle activity, we used the aerodynamic power model implemented in the R package afpt (40) based on Pennycuick (38) and Klein Heerenbrink et al. (39). Mechanical power displays a U-shaped curve as a function of flight speed (37, 38), and the speed that minimizes this curve (i.e., the minimum power speed) is typically selected by bats for short flights and feeding (27). We used the aerodynamic model to calculate the minimum power speed and the mechanical work for flapping, W_{flight}. Then, considering the conversion efficiency of flight muscles between chemical energy and mechanical, η, the energy cost of flight was estimated as W_{flight}/η (where $\eta = 0.23$; see ref. 38). Finally, to estimate the amount of heat generated as a by-product of flapping, Q_{flight}, we used the definition of muscle efficiency by Hill (55), where $\eta = W_{flight}/(W_{flight} + Q_{flight})$. Therefore, we assume that η is a constant independent of size and that all chemical energy is either transformed into work or heat. Although these assumptions oversimplify the actual mechanisms driving energy conversion in vertebrates (56–58), the overall effect of the activity–thermoregulation heat substitution on the model's predictions was low, and thus the main predictions did not depend on these assumptions (*SI Appendix*, section 3). Finally, we validated the model's predictions using both thermogenic metabolic rates measured in a respirometer for 5 species of bats and field metabolic rates of 16 species of bats (*SI Appendix*, section 2).

Data Collection and Analyses. To test the model's predictions on the mode of evolution of wing S-MR in bats, we used empirical data from 278 species from 17 families. We collected data on wing surface area, body mass, and wingspan of each species (27). We also collected environmental temperatures for each species using the mean annual temperature from Worldclim 2.1 (59). We extracted the median temperature for each species based on their geographic distributions from IUCN redlist (60). The annual temperature across the geographic distribution may not accurately describe the experienced environmental conditions of 48 species (17%) that are known to migrate or suspected of migration (61). However, the migratory range of these species has not been characterized, and it remains poorly understood whether they exhibit partial migration (i.e., only part of their population migrate) or even facultative migration [i.e., individuals can migrate or remain sedentary depending on local cues like resource availability (61)]. Therefore, to avoid reducing the sample size of our phylogenetic models, we did not exclude these species and characterized their environmental temperature in the same way as for nonmigratory species. Finally, we accounted for the phylogenetic relatedness among species using the phylogeny by Kuhn et al. (62). Seven species missing in the phylogeny were randomly inserted in their genus using functions implemented in the phytools R package (63).

To analyze the mode of evolution of S-MR, we compared the goodness of fit of BM and OU models. While the BM model assumes that the trait evolves gradually and the variance increases linearly with time, the OU model assumes that the trait is continuously pulled back toward an optimum value, lowering the trait variance. The OU model can incorporate different optimal trait values, θ, variances, σ^2, and strengths of selection, α, thus capturing differences in the selective regime across environments (64). We used this multioptimum OU model to test whether the strength of selection and variance is higher among species living in cold environments. Although our biophysical model predicts gradual changes in response to temperature, the OU model uses discrete optima. We, therefore, categorized our temperature gradient using quantiles: i.e., hot-living (first quartile), midtemperature (second and third quartile), or cold-living species (fourth quartile). To avoid potential artifacts due to arbitrary categorization of temperature in three groups, we also categorized species in two groups, i.e., either below or above the median temperature, 24.7 °C. Each multioptimum OU model was fitted with either three or two temperature categories. We compared the candidate models: 1) temperature-independent, neutral Brownian motion model (BM1); 2) temperature-dependent BM, allowing the evolutionary rate parameter (σ^2) to differ among temperature levels (BM2); 3) temperature-independent OU model with a single attractor (OU1); 4) temperature-dependent OU model allowing optimum S-MR (θ) to vary among temperature levels while keeping constant evolutionary rate (σ^2) and strength of selection (α) (OU2); 5) temperature-dependent OU model with free θ and σ^2 and keeping α as a constant (OU3); and 6) temperature-dependent OU model with all free parameters θ, σ^2, α (OU4). The selection of candidate models was performed using the Akaike's information criterion corrected for small sample sizes (AICc). Analyses were performed using the packages OUwie (64) and phytools (63) in R 3.2 (65).

Data Availability. CSV dataset and R code have been deposited in Zenodo (https://zenodo.org/record/6350431#.YjI5ZnrMKUk).

Author affiliations: [a]Department of Biology, McGill University, Montreal, QC H3A 1B1, Canada; [b]Departamento de Biología y Geología, Física y Química Inorgánica, Universidad Rey Juan Carlos, 28933 Madrid, Spain; [c]Departamento de Ecologia, Universidade Federal de Sergipe, 49100-000 Sergipe, Brazil; [d]Red de Biología Evolutiva, Instituto de Ecología A.C., 91070 Xalapa, Mexico; [e]Departamento de Biodiversidade, Instituto de Biociências, Universidade Estadual Paulista Júlio de Mesquita Filho, 13506-900 São Paulo, Brazil; [f]Departamento de Biologia, Universidade Federal de Sergipe, 49100-000 Sergipe, Brazil; [g]Departamento de Fisiologia, Instituto de Biociência, Universidade de São Paulo, 05508-090 São Paulo, Brazil; [h]Instituto de Biologia, Universidade Federal da Bahia, 40170-115 Salvador, BA, Brazil; and [i]Departamento de Ecologia, Instituto de Ciências Biológicas, Universidade Federal de Goiás, 74001-970 Goiânia, Brazil

1. M. Kleiber, Body size and metabolism. *Hilgardia* **6**, 315–353 (1932).
2. R. H. Peters, K. Wassenberg, The effect of body size on animal abundance. *Oecologia* **60**, 89–96 (1983).
3. K. Schmidt-Nielsen, S. N. Knut, *Scaling: Why Is Animal Size So Important?* (Cambridge University Press, 1984).
4. B. K. McNab, The economics of temperature regulation in neotropical bats. *Comp. Biochem. Physiol.* **31**, 227–268 (1969).
5. B. K. McNab, *Extreme Measures: The Ecological Energetics of Birds and Mammals* (University of Chicago Press, 2012).
6. J. H. Brown, Macroecology: Progress and prospect. *Oikos* **87**, 3–14 (1999).
7. A. R. Evans *et al.*, The maximum rate of mammal evolution. *Proc. Natl. Acad. Sci. U.S.A.* **109**, 4187–4190 (2012).
8. S. F. Gouveia *et al.*, Ecophysics reload–Exploring applications of theoretical physics in macroecology. *Ecol. Modell.* **424**, 109032 (2020).
9. T. E. Higham *et al.*, Linking ecomechanical models and functional traits to understand phenotypic diversity. *Trends Ecol. Evol.* **36**, 860–873 (2021).
10. C. Bergmann, Über die verhältnisse der wärmeökonomie der thiere zu ihrer grösse. *Gött. Stud.* **3**, 595–708 (1847).
11. M. Á. Rodríguez, M. Á. Olalla-Tárraga, B. A. Hawkins, Bergmann's rule and the geography of mammal body size in the Western Hemisphere. *Glob. Ecol. Biogeogr.* **17**, 274–283 (2008).
12. V. A. Olson *et al.*, Global biogeography and ecology of body size in birds. *Ecol. Lett.* **12**, 249–259 (2009).
13. J. A. Allen, The influence of physical conditions in the genesis of species. *Rad. Rev.* **1**, 108–140 (1877).
14. M. R. Symonds, G. J. Tattersall, Geographical variation in bill size across bird species provides evidence for Allen's rule. *Am. Nat.* **176**, 188–197 (2010).
15. T. M. Blackburn, K. J. Gaston, N. Loder, Geographic gradients in body size: A clarification of Bergmann's rule. *Divers. Distrib.* **5**, 165–174 (1999).
16. D. Pincheira-Donoso, The balance between predictions and evidence and the search for universal macroecological patterns: Taking Bergmann's rule back to its endothermic origin. *Theory Biosci.* **129**, 247–253 (2010).
17. B. K. McNab, Geographic and temporal correlations of mammalian size reconsidered: A resource rule. *Oecologia* **164**, 13–23 (2010).
18. V. Millien *et al.*, Ecotypic variation in the context of global climate change: Revisiting the rules. *Ecol. Lett.* **9**, 853–869 (2006).
19. T. S. Fristoe *et al.*, Metabolic heat production and thermal conductance are mass-independent adaptations to thermal environment in birds and mammals. *Proc. Natl. Acad. Sci. U.S.A.* **112**, 15934–15939 (2015).
20. W. Bogdanowicz, Geographic variation and taxonomy of Daubenton's bat, *Myotis daubentoni* in Europe. *J. Mammal.* **71**, 205–218 (1990).

21. S. Meiri, T. Dayan, On the validity of Bergmann's rule. *J. Biogeogr.* **30**, 331–351 (2003).

22. L. A. V. D. de Barros, R. D. R. Fortes, M. L. Lorini, The application of Bergmann's rule to *Carollia perspicillata* (Mammalia, Chiroptera). *Chirop. Neotrop.* **20**, 1243–1251 (2014).

23. K. Safi, S. Meiri, K. E. Jones, "Evolution of body size in bats" in *Animal Body Size: Linking Pattern and Process across Space, Time, and Taxonomic Group*, F. A. Smith, S. K. Lyons, Eds. (The University of Chicago Press, 2013), pp. 95–151.

24. J. Gohli, K. L. Voje, An interspecific assessment of Bergmann's rule in 22 mammalian families. *BMC Evol. Biol.* **16**, 222 (2016).

25. J. M. V. Rayner, Biomechanical constraints on size in flying vertebrates. *Symp. Zool. Soc. Lond.* **69**, 83–109 (1996).

26. N. Cooper, A. Purvis, Body size evolution in mammals: Complexity in tempo and mode. *Am. Nat.* **175**, 727–738 (2010).

27. U. M. Norberg, J. M. Rayner, Ecological morphology and flight in bats (Mammalia; Chiroptera): Wing adaptations, flight performance, foraging strategy and echolocation. *Philos. Trans. R. Soc. Lond., B* **316**, 335–427 (1987).

28. J. R. Speakman, G. C. Hays, P. I. Webb, Is hyperthermia a constraint on the diurnal activity of bats? *J. Theor. Biol.* **171**, 325–339 (1994).

29. J. D. Reichard, S. I. Prajapati, S. N. Austad, C. Keller, T. H. Kunz, Thermal windows on Brazilian free-tailed bats facilitate thermoregulation during prolonged flight. *Integr. Comp. Biol.* **50**, 358–370 (2010).

30. J. R. Speakman, D. W. Thomas, T. H. Kunz, M. B. Fenton, "Physiological ecology and energetics of bats" in *Bat Ecology*, T. H. Kunz, M. B. Fenton, Eds. (The University of Chicago Press, 2003), pp. 430–490.

31. J. R. Speakman, E. Król, Maximal heat dissipation capacity and hyperthermia risk: Neglected key factors in the ecology of endotherms. *J. Anim. Ecol.* **79**, 726–746 (2010).

32. J. H. Brown, W. A. Calder, III, A. Kodric-Brown, Correlates and consequences of body size in nectar-feeding birds. *Am. Zool.* **18**, 687–738 (1978).

33. U. M. Norberg, Evolutionary convergence in foraging niche and flight morphology in insectivorous aerial-hawking birds and bats. *Ornis Scand.* **17**, 253–260 (1986).

34. U. M. L. Norberg, R. Å. Norberg, Scaling of wingbeat frequency with body mass in bats and limits to maximum bat size. *J. Exp. Biol.* **215**, 711–722 (2012).

35. W. P. Porter, J. C. Munger, W. E. Stewart, S. Budaraju, J. Jaeger, Endotherm energetics-from a scalable individual-based model to ecological applications. *Aust. J. Zool.* **42**, 125–162 (1994).

36. W. P. Porter, M. Kearney, Size, shape, and the thermal niche of endotherms. *Proc. Natl. Acad. Sci. U.S.A.* **106** (suppl. 2), 19666–19672 (2009).

37. C. J. Pennycuick, *Bird Flight Performance* (Oxford University Press, 1989).

38. C. J. Pennycuick, *Modelling the Flying Bird* (Elsevier, 2008).

39. M. Klein Heerenbrink, L. C. Johansson, A. Hedenström, Power of the wingbeat: Modelling the effects of flapping wings in vertebrate flight. *Proc. Roy. Soc. A* **471**, 20140952 (2015).

40. M. Klein Heerenbrink, afpt: Tools for modelling of animal flight performance. R package (Version 1.1.0.1. https://cran.r-project.org/web/packages/afpt/index.html, 2020).

41. R. McN. Alexander, *Optima for Animals* (Princeton University Press, 1996).

42. W. C. Lancaster, S. C. Thomson, J. R. Speakman, Wing temperature in flying bats measured by infrared thermography. *J. Therm. Biol.* **22**, 109–116 (1997).

43. J. D. Reichard, S. R. Fellows, A. J. Frank, T. H. Kunz, Thermoregulation during flight: body temperature and sensible heat transfer in free-ranging Brazilian free-tailed bats (*Tadarida brasiliensis*). *Physiol. Biochem. Zool.* **83**, 885–897 (2010).

44. C. P. Lyman, *Hibernation and Torpor in Mammals and Birds* (Elsevier, 2013).

45. A. P. Cruz-Neto, F. Bozinovic, The relationship between diet quality and basal metabolic rate in endotherms: Insights from intraspecific analysis. *Physiol. Biochem. Zool.* **77**, 877–889 (2004).

46. A. P. Cruz-Neto, L. G. M. Herrera, "The relationship between physiology and diet" in *Phyllostomid Bats: A Unique Mammalian Radiation*, T. H. Fleming, L. M. Dávalos, M. A. Mello, Eds. (The University of Chicago Press, 2020), pp. 169–186.

47. R. D. Stevens, Historical processes enhance patterns of diversity along latitudinal gradients. *Proc. Biol. Sci.* **273**, 2283–2289 (2006).

48. F. P. Peixoto, F. Villalobos, M. V. Cianciaruso, Phylogenetic conservatism of climatic niche in bats. *Glob. Ecol. Biogeogr.* **26**, 1055–1065 (2017).

49. S. K. Lyons, M. R. Willig, Species richness, latitude, and scale-sensitivity. *Ecology* **83**, 47–58 (2002).

50. M. J. Ramos Pereira, J. M. Palmeirim, Latitudinal diversity gradients in New World bats: Are they a consequence of niche conservatism? *PLoS One* **8**, e69245 (2013).

51. H. T. Arita, J. Vargas-Barón, F. Villalobos, Latitudinal gradients of genus richness and endemism and the diversification of New World bats. *Ecography* **37**, 1024–1033 (2014).

52. M. C. Urban *et al.*, Improving the forecast for biodiversity under climate change. *Science* **353**, aad8466 (2016).

53. E. L. Rezende, L. D. Bacigalupe, Thermoregulation in endotherms: Physiological principles and ecological consequences. *J. Comp. Physiol. B* **185**, 709–727 (2015).

54. M. M. Humphries, V. Careau, Heat for nothing or activity for free? Evidence and implications of activity-thermoregulatory heat substitution. *Integr. Comp. Biol.* **51**, 419–431 (2011).

55. A. V. Hill, The heat of shortening and the dynamic constants of muscle. *Proc. R. Soc. Lond. B Biol. Sci.* **126**, 136–195 (1938).

56. E. Gnaiger, J. M. Shick, J. Widdows, "Metabolic microcalorimetry and respirometry of aquatic animals" in *Techniques in Comparative Respiratory Physiology: An Experimental Approach*, C. R. Bridges, P. J. Butler, Eds. (Cambridge University Press, 1989), pp. 113–135.

57. C. P. Ellington, Power and efficiency of insect flight muscle. *J. Exp. Biol.* **115**, 293–304 (1985).

58. S. Ward *et al.*, Metabolic power of European starlings *Sturnus vulgaris* during flight in a wind tunnel, estimated from heat transfer modelling, doubly labelled water and mask respirometry. *J. Exp. Biol.* **207**, 4291–4298 (2004).

59. S. E. Fick, R. J. Hijmans, WorldClim 2: New 1km spatial resolution climate surfaces for global land areas. *Int. J. Climatol.* **37**, 4302–4315 (2017).

60. IUCN, The IUCN red list of threatened species. 2020.1. https://www.iucnredlist.org. Accessed 7 June 2020.

61. J. J. Krauel, G. F. McCracken, "Recent advances in bat migration research" in *Bat Evolution, Ecology, and Conservation*, R. A. Adams, S. C. Pedersen, Eds. (Springer Science Press, 2013), pp. 293–314.

62. T. S. Kuhn, A. Ø. Mooers, G. H. Thomas, A simple polytomy resolver for dated phylogenies. *Methods Ecol. Evol.* **2**, 427–436 (2011).

63. L. J. Revell, phytools: An R package for phylogenetic comparative biology (and other things). *Methods Ecol. Evol.* **3**, 217–223 (2012).

64. J. M. Beaulieu, D. C. Jhwueng, C. Boettiger, B. C. O'Meara, Modeling stabilizing selection: Expanding the Ornstein-Uhlenbeck model of adaptive evolution. *Evolution* **66**, 2369–2383 (2012).

65. R Core Team, *R: A Language and Environment for Statistical Computing* (R Foundation for Statistical Computing, Vienna, 2019).